Journal of Catalysis 273 (2010) 221–228

Contents lists available at ScienceDirect

Journal of Catalysis

journal homepage: www.elsevier.com/locate/jcat

Characterization and reactivity of sol–gel synthesized TiO_2–Al_2O_3 supported vanadium oxide catalysts

Debaprasad Shee [a], Goutam Deo [a,*], Andrew M. Hirt [b]

[a] Department of Chemical Engineering, Indian Institute of Technology Kanpur, Kanpur 208 016, India
[b] Materials Research Laboratories, Inc., Struthers, OH 44471, USA

ARTICLE INFO

Article history:
Received 6 March 2010
Revised 24 May 2010
Accepted 24 May 2010
Available online 3 July 2010

Keywords:
TiO_2–Al_2O_3 support
Vanadium oxide
Raman
Diffuse reflectance Fourier transformed infrared spectroscopy (DRIFT)
X-ray photoelectron spectroscopy (XPS)
Kinetic parameter
Propane oxidative dehydrogenation (ODH)

ABSTRACT

A 90 wt% TiO_2 in a titania–alumina mixed oxide support (90Ti–Al) was synthesized by the sol–gel method and characterized. Several 90Ti–Al supported vanadium oxide (vanadia) catalysts, *x*V90Ti–Al, were also synthesized, characterized and probed by the propane oxidative dehydrogenation (ODH) reaction. For the 90Ti–Al support and low vanadia loadings, no rutile peak was observed even after calcination at 1073 K. For vanadia loading greater than 7.5 wt%, rutile peaks were observed at 923 K and higher calcination temperatures. Characterization and reactivity studies suggest that molecularly dispersed, reducible surface vanadia species are present and active for the propane ODH reaction. However, the presence of alumina on the support surface decreased the catalytic activity relative to only titania. The activity variation with calcination temperature had a pronounced effect on the activity of some catalysts and is related to the presence/absence of the surface vanadia species and the surface Al/Ti ratio, both of which change with calcination temperature.

1. Introduction

Supported vanadium oxide (vanadia) is a commonly used catalyst for various selective catalytic oxidation and reduction processes [1–6]. The reactivity of supported vanadia catalysts for a particular reaction depends on vanadia loading and the specific oxide support apart from other parameters [7,8]. The surface structure of vanadium oxide dispersed on various supports depends on the vanadia loading and support and are extensively studied by various characterization techniques ([7] and reference therein). Furthermore, the nature of the surface vanadia species appears to be sensitive to the calcination temperature [9,10].

It is proposed that the vanadia catalyst supported on anatase titania is more active and selective for selective catalytic oxidation and reduction reactions [7]. However, the major disadvantages associated with the titania support are its relatively low surface area and rapid sintering that occurs at high temperatures. Furthermore, the presence of vanadia in the supported catalysts accelerates the sintering process and the anatase to rutile phase transformation. To overcome these shortcomings, several studies were targeted at obtaining titania-based mixed oxide supports of high surface area and thermal stability ([7] and reference therein). These titania-based mixed oxide supports are obtained by combining titania with another thermally stable and high surface area metal oxide [7]. Alumina and silica are commonly used thermally stable large surface area material possessing good mechanical properties [11]. It has been reported that incorporating small amounts of these metal oxides (<10 mol%) improves the thermal stability of the titania-based supports. The improvement in thermal stability is achieved by retarding the anatase to rutile transformation [12]. Other support-related properties are also improved. Change in oxygen vacancy concentration, formation of solid solution and exo-solution process from the solid solution to rutile and dopant oxide are a few of the many mechanisms proposed for the delayed transformation of anatase to rutile in the presence of a dopant oxide [13–15]. Of the various titania-based mixed oxide supports, the titania–alumina mixed oxides are used for various petrochemical processes. These titania–alumina mixed oxide supports can be synthesized by various methods [16–18]. Furthermore, synthesis of catalytic material by sol–gel method is of great interest since this method provides a great degree of control over molecular-scale mixing.

In the present study, a titania–alumina mixed oxide support containing small amount of alumina is synthesized by the sol–gel method. Using this synthesized support, several supported vanadia catalysts are prepared by the incipient wetness impregnation method and characterized. The catalytic activity of these supported vanadia catalysts is probed by the propane ODH reaction. The propane ODH reaction was chosen as a probe reaction for this catalytic

* Corresponding author. Fax: +91 512 2590104.
E-mail address: goutam@iitk.ac.in (G. Deo).

0021-9517/$ - see front matter © 2010 Elsevier Inc. All rights reserved.
doi:10.1016/j.jcat.2010.05.017

system since this reaction has been extensively studied at one of our laboratories [8,19–24]. To obtain further understanding of this catalytic system, the effect of calcination temperature on the nature of the vanadia supported on the mixed oxide support was also undertaken.

2. Experimental

2.1. Material synthesis

The TiO_2–Al_2O_3 mixed oxide support containing 90 wt% TiO_2 was prepared by the sol–gel method based on published protocol ([25] and reference therein). The precursors used for titania and alumina were titanium ethoxide (Sigma–Aldrich, 98% purity) and aluminum-tri-sec-butoxide (ATSB, Sigma–Aldrich, 97% purity), respectively. Cetyltrimethylammonium bromide (CTAB) was used as a template/surfactant. Specifically, a measured amount of titanium ethoxide precursor was added to a mixture of CTAB and absolute ethanol (99.99%). The resulting mixture was stirred for 45 min. The required amount of ATSB was then added to this mixture. The hydrolyzing agent used in this particular synthesis was a mixture of HNO_3 and H_2O in known amounts. The hydrolyzing agent was added drop wise to the continuously stirred precursor mixture until complete hydrolysis. After sometime, a gel was formed, which was aged for 24 h. The molar ratio of titanium ethoxide, ATSB, CTAB, HNO_3, H_2O and ethanol in the final mixture was 1:0.17:0.2:1.5:10:20. After completion of aging, a mixture of NH_4OH and double distilled water was added to the gel. The mixture was refluxed at 353 K for 48 h, and the pH of the mixture was maintained between 9 and 10 during the reflux period. The white precipitate obtained was filtered and dried overnight in a vacuum desiccator. The white cake was then dried at 333 K for 8 h followed by drying at 383 K for 6 h. The dried cake was then ground to powder and calcined at 723 K to make the final mixed oxide support. The support was denoted as 90Ti–Al.

The 90Ti–Al supported vanadia catalysts of various loading (2–10 wt% V_2O_5) were synthesized by the incipient wetness impregnation method using ammonium metavanadate as the vanadia precursor. For higher loading samples, multiple impregnation technique was used. The details of the catalyst synthesis are given elsewhere [19]. The final catalyst was calcined at 723 K. The catalyst was denoted as *x*V90Ti–Al, where x represents the wt% of vanadia as V_2O_5 present in the catalysts. The final calcination temperature was chosen as 723 K since temperatures in excess of 773 K may lead to the transformation of the anatase to rutile phase of titania, especially in the presence of vanadia. Higher calcination temperatures appear to deactivate the catalyst [10]. The catalysts were also calcined at higher temperatures to study the effect of calcination temperature and to observe whether deactivation takes place.

2.2. Surface area measurement

The surface areas of the samples were determined by nitrogen adsorption method using the single point Brunauer–Emmett–Teller (BET) equation. A 30% N_2/He gas mixture was used for adsorption. In the present study, a SMART SORB 92/93 BET surface area analyzer was used for BET surface area measurements. Degassing was achieved by heating the sample at 473 K followed by flushing with carrier gas before adsorption of nitrogen at 77 K.

2.3. X-ray diffraction (XRD)

The XRD patterns of all the samples were obtained in the range of 10–70° with a scanning speed of 3° min^{-1} on an ISO Debye flex-2002 X-ray diffractometer using Cu Kα irradiation (λ = 1.54056 Å).

2.4. Raman spectroscopy

Raman spectra of the 90Ti–Al support and *x*V90Ti–Al catalysts were obtained under ambient and dehydrated conditions using an ultraviolet (UV)-visible Raman spectrometer system (Horiba-Jobin Yvon LabRam-HR) equipped with a confocal microscope containing 2400/900 grooves/mm grating and a notch filter. A 532-nm (Visible) Yag double-diode pumped laser source was used for the excitation of the samples. All the spectra were taken at a resolution of ~2 cm^{-1}. To obtain the spectra under dehydrated conditions, the powdered samples were placed in a high temperature *in situ* cell (Linkam THMS-1600). The samples were treated at 673 K in a flowing stream of 10% O_2 in Ar for 30 min before the Raman spectra were taken. Additional details are given elsewhere [26].

2.5. Diffuse reflectance Fourier transformed infrared (DRIFT) spectroscopy

The DRIFT spectra of the dehydrated 90Ti–Al support and *x*V90Ti–Al (x = 2–10 wt%) catalysts were recorded on a BRUKER TENSOR 27 FTIR spectrometer attached with a diffuse reflectance accessory (HARRICK Praying Mantis, DRP-BR4) and a high temperature reaction chamber (HARRICK HVC-DRP-2) equipped with KBr windows. To obtain the spectra under dehydrated conditions, the powder sample placed in the sample cup of the reaction chamber and oxygen gas at a flow rate of 30 ml/min was introduced into the reaction chamber. Before recording the spectra, the reaction chamber containing the catalyst sample was heated at 673 K for 45 min by an automatic temperature controller module (HARRICK ATC-024-2). All spectra were collected at a resolution of 4 cm^{-1} using 128 scan. Each spectrum was subtracted from a KBr background collected under conditions similar to that of the sample.

2.6. Temperature-programmed reduction (TPR) studies

TPR studies of *x*V90Ti–Al catalysts were carried out in a Micromeritics Pulse Chemisorb 2705 apparatus. Samples of 25–35 mg were loaded into a U-tube quartz reactor. Prior to the reduction process, all the samples were pre-treated at 473 K for 30 min in a stream of Ar gas flowing at a rate of 30 ml/min to remove adsorbed moisture and any other adsorbed impurities that may be present. The reactor was then cooled to room temperature, and a mixture of 5% H_2–Ar gas flowing at a rate of 30 ml/min was introduced into the quartz reactor. The reactor was heated to 1200 K using a temperature-programmed rate of 10 K/min. The hydrogen consumption was monitored by a thermal conductivity detector.

2.7. Reaction studies and kinetic parameter estimation

The catalytic activity of the *x*V90Ti–Al catalysts was tested for the propane ODH reaction. The ODH reaction was carried out in a fixed bed, down flow, isothermal tubular quartz reactor at atmospheric pressure. Three separate mass flow controllers (Bronkhost Hi-Tech, E1 mass flow controller) controlled the inlet gas (propane, nitrogen and oxygen) flow rates. Two types of reactivity data were collected for the propane ODH reaction: contact time and kinetic parameter estimation related data. For contact time related data, the total inlet gas flow rate was varied from 30 to 120 ml/min; and for kinetic parameter estimation related data, a total inlet gas flow rate of 75 ml/min was used. Contact time related data were obtained at a reaction temperature of 653 K using propane to oxygen molar ratio of 2:1. For kinetic parameter estimation related data, the reaction temperature was varied from 613 to 673 K, and the propane to oxygen molar ratio was varied from 1:1 to 3:1. Nitrogen was used as a diluent during reaction, and its quantity

was adjusted with oxygen such that the inlet nitrogen and oxygen composition corresponds to that of air. The propane conversion for all reactivity studies was maintained below 10% to ensure minimal mass and heat transfer effects. Blank experiments were also carried out at identical reaction conditions to confirm the absence of homogeneous reaction. Additional details of the reactor setup, calculations for conversion, selectivity, yield and kinetic parameters estimation can be found elsewhere [19–21].

2.8. X-ray photoelectron spectroscopy (XPS) studies

For XPS analysis, the samples were attached to stainless steel holders using conductive double-sided carbon tape and then installed in the vacuum chamber of a Model DS800 XPS surface analysis system manufactured by Kratos Analytical Plc of Manchester, UK. The chamber was evacuated to a base pressure of $\approx 5 \times 10^{-9}$ torr. A hemispherical energy analyzer was used for electron detection. XPS survey spectra were collected to identify the elements present on the sample surfaces, and high-resolution spectra were collected to indicate the chemical structures present. The obtained spectra were plotted and used to generate estimates of the atomic and weight concentrations of the elements indicated by the peaks present in the spectral data. Data were collected using a magnesium K-alpha X-ray source and 80 or 40 eV pass energy settings in the fixed analyzer transmission mode. Elements were identified in each spectrum, and the concentrations were estimated using typical normalization procedures. Sensitivity factors employed were selected based on the peak envelope measured for each element of interest: Ti 2p and Al 2p (entire envelope) and the V $2p_{3/2}$ (only, to avoid O peak interferences). Since the carbon concentrations were relatively low, and the kinetic energy positions of the peaks of interest were similar for the elements of interest, the effect of carbon over layer presence was ignored in this study [27]. The mean free paths of the electrons for vanadium and titanium are very similar so quantitative data for these elements will likely be quite accurate. The mean free path for the aluminum signals is longer and may result in a slight overestimate of aluminum content relative to the V and Ti. For the purposes of this study, only the changes in relative composition are important; not the absolute accuracy of the calculated concentrations.

3. Results and discussion

3.1. Characterization of titania–alumina support and supported vanadia catalysts

The surface area of the 90Ti–Al support and the *x*V90Ti–Al (*x* = 2–10 wt%) catalysts calcined at 723 K were determined and presented in Table 1. The T_{max} value obtained from TPR studies and the CO_2/CO ratio, ψ, obtained from reaction studies are also tabulated in Table 1 and are discussed later. A surface area of 113 m^2/g was achieved for the 90Ti–Al support, which decreased with an increase in vanadia loading in the *x*V90Ti–Al samples. The surface density of vanadia based on the pure 90Ti–Al support surface area is also presented in Table 1 and varied from 1.2 to 6.5 V atoms/nm^2. The surface density of vanadia was lower than reported monolayer limits of supported vanadia catalysts [28].

Table 1
Surface area, surface vanadia density, T_{max} and ψ of the *x*V90Ti–Al catalysts.

Nomenclature	V_2O_5 (wt%)	Surface area (m^2/g)	Surface density (V atoms/nm^2)	T_{max} (K)	CO_2/CO[a] ψ
90Ti–Al	–	113	–	835	–
2V90Ti–Al	2	91	1.2	721	0.37
4V90Ti–Al	4	93	2.4	737	0.27
7.5V90Ti–Al	7.5	83	4.8	749	0.16
10V90Ti–Al	10	73	6.5	755	0.14

[a] Based on entire reaction data.

With an increase in calcination temperature, the surface area of the 90Ti–Al support and *x*V90Ti–Al catalysts (*x* = 2–10 wt%) was observed to decrease for all samples. To compare the relative decrease in surface areas, the normalized surface area values were determined. Normalization is achieved by dividing the surface area of a sample calcined at a particular temperature to the surface area of the same sample calcined at 723 K. Thus, the normalized surface area of the 90Ti–Al support and *x*V90Ti–Al catalysts calcined at 723 K is unity. The normalized surface areas versus calcination temperature for the different samples are shown in Fig. 1. Fig. 1 shows that the 90Ti–Al support retains ~40% of the initial surface area at 1023 K. In comparison, TiO_2 (P25, Degussa) does not retain much of its initial surface area at 1023 K. Pure titania synthesized using a similar method also lost its surface area at higher calcination temperatures more rapidly than the 90Ti–Al mixed oxide support. The results for the pure TiO_2 support synthesized by a similar method are not shown for brevity. In the presence of vanadia, the relative decrease in surface area with calcination temperature is larger, which progressively becomes more significant for higher vanadia loading samples. Reddy et al. observed similar variations in surface area with calcination temperature for a similar system [7].

The 90Ti–Al support and *x*V90Ti–Al catalysts calcined at different temperatures were also characterized by XRD. The XRD patterns of 90Ti–Al support calcined at different temperatures reveal the absence of the rutile phase even up to a calcination temperature of 1073 K as shown in Fig. 2. The rutile phase was also not observed for 2V90Ti–Al and 4V90Ti–Al at 1073 K, and the XRD patterns were not shown for brevity. For 7.5V90Ti–Al, the rutile phase appears at 973 K, and the anatase phase does not completely disappear even at a calcination temperature of 1073 K. For 10V90Ti–Al, the rutile phase is initially observed at 923 K, and it is the only phase observed at 973 K. Furthermore, an additional peak ($2\theta = 21.7°$) for crystalline V_2O_5 [29] appears at 973 K for 10V90Ti–Al. It appears that at high calcination temperatures bulk V_2O_5 is formed in the 10V90Ti–Al sample. From the earlier discussion, it is also evident that the anatase to rutile phase transformation occurs in the vanadia-based samples containing more than 4% V_2O_5 at progressively lower calcination temperatures. The lower anatase to rutile transformation temperature observed in the high

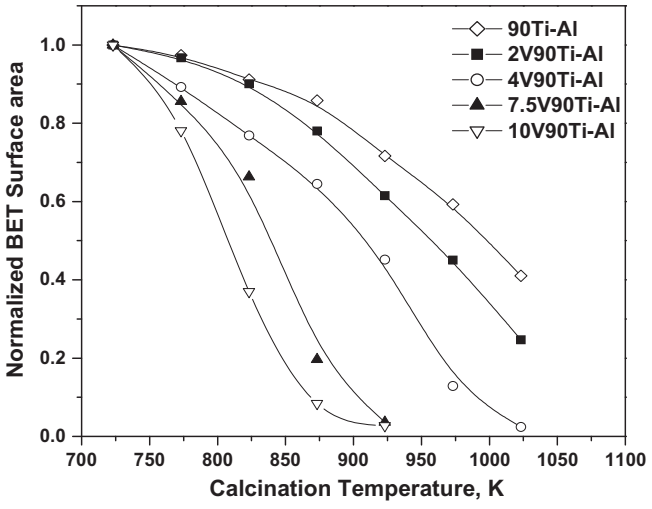

Fig. 1. Variation of surface area with calcination temperature for *x*V90Ti–Al catalysts.

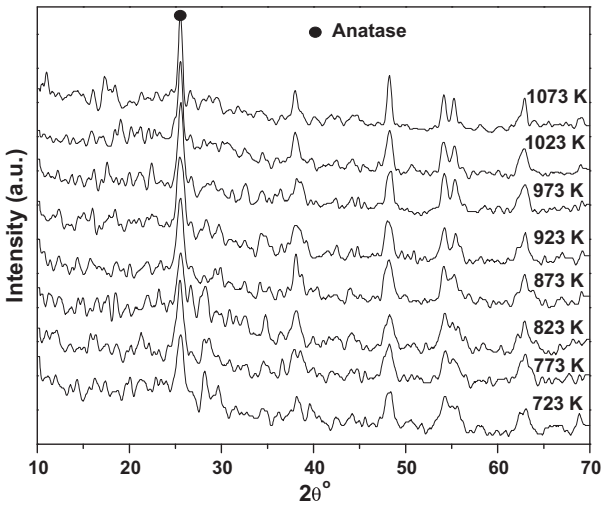

Fig. 2. XRD patterns of 90Ti–Al support calcined at different temperatures.

vanadia containing samples has been proposed to be due to: (i) the high mobility of V in the structure, (ii) incorporation of V in the titania anatase structure and (iii) introduction of distortion [15,30].

The Raman spectra of 90Ti–Al and *x*V90Ti–Al were obtained under ambient and dehydrated conditions. The Raman spectra of the dehydrated samples are shown in Fig. 3 in the 750–1100 cm^{-1} region. The spectra obtained under ambient condition are not shown for brevity. Fig. 3 reveals a Raman band at 1030 cm^{-1} due to the terminal V=O bond vibration of surface molecularly dispersed vanadia species, and the intensity of this band increases with an increase in vanadia loading [31–35]. An additional broad feature at 935 cm^{-1} was observed for 7.5 wt% vanadia loading and above. Appearance of the 935 cm^{-1} band suggests the presence of polymeric surface vanadia species or support associated vibrations of the surface vanadia species [31–36]. The Raman spectra of the different samples reveal that only molecularly dispersed surface vanadia species are present on this mixed oxide support and, as expected, the monolayer coverage is not achieved until 10 wt% of vanadia loading.

The DRIFT spectra of the *x*V90Ti–Al samples were obtained under dehydrated conditions. The spectra of the dehydrated *x*V90Ti–Al samples shown in Fig. 4 reveal a band at 2035 cm^{-1}, which is assigned to the V=O bond overtone vibration [37]. The intensity of the overtone band continuously increases with an increase in vanadia loading. Changes in the hydroxyl region, 4000–3300 cm^{-1}, are also observed and are shown in Fig. 5. The 90Ti–Al support reveals IR bands at 3770, 3730, 3676 and 3650–3635 cm^{-1}. The first three bands are assigned to basic, neutral and acidic OH groups of alumina [38]. The IR band at 3676 cm^{-1} is also assigned to the isolated hydroxyl group vibration of titania, and the band at 3650–3635 cm^{-1} is assigned to the bridged hydroxyl group vibration of titania [38]. The band at 3770 cm^{-1} is titrated even at the lowest vanadia loading. The intensities of the 3730, 3676 and the broad band at 3650–3635 cm^{-1} bands also decreases with vanadia loading and are still present for the 10V90Ti–Al sample. The presence and gradual disappearance of the titania and alumina hydroxyls with vanadia loading suggests that titania and alumina are present on the surface of the mixed oxide support synthesized in the present study and coordinate with the surface vanadia species. The preferential titration of the

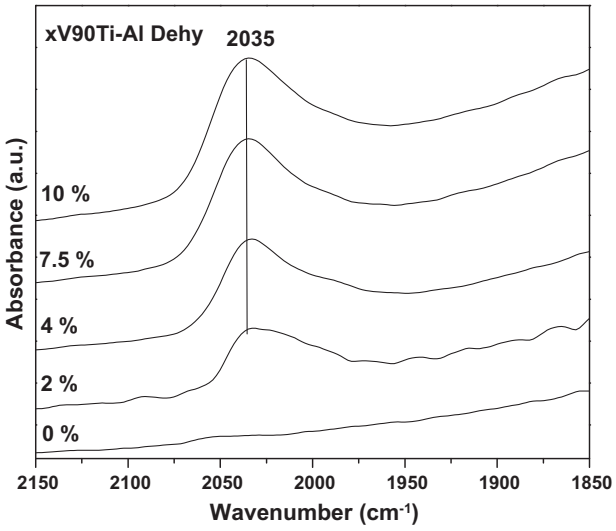

Fig. 4. IR spectra of the *x*V90Ti–Al catalysts (*x* = 0–10 wt%) in metal oxygen region under dehydrated conditions.

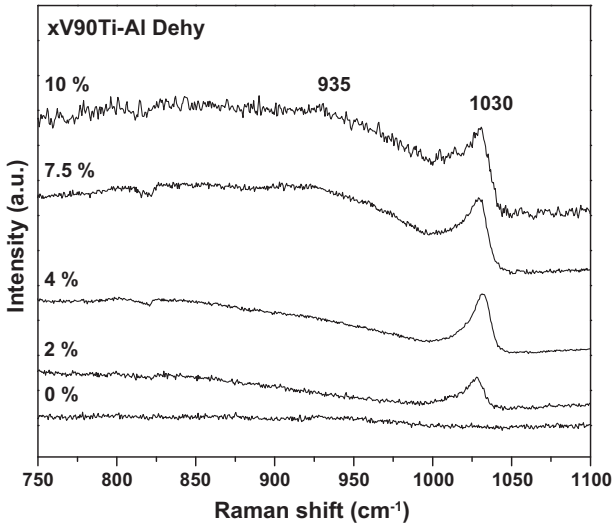

Fig. 3. Raman spectra of *x*V90Ti–Al catalysts (*x* = 0–10 wt%) obtained under dehydrated conditions.

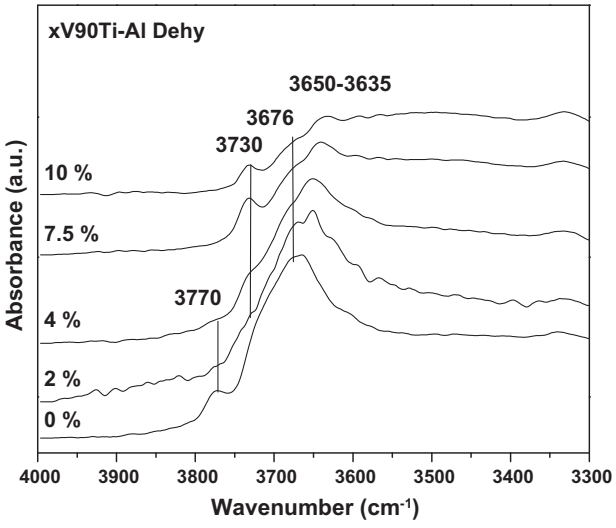

Fig. 5. IR spectra of the *x*V90Ti–Al catalysts ((*x* = 0–10 wt%) in hydroxyl region under dehydrated conditions.

titania hydroxyl group versus the alumina hydroxyl group is not evident.

The TPR results obtained for all samples are shown in Fig. 6, and the T_{max} values are tabulated in Table 1. The TPR result for 90Ti–Al is included as a reference and shows a minor reduction peak at 835 K. The TPR profile of each *x*V90Ti–Al catalyst reveals a distinct reduction peak in the 721–755 K region. The reduction peak observed in the 721–755 K region is due to the reduction of surface vanadia species, and it shifts to higher temperatures as vanadia loading is increased. In comparison, the reduction peak for V_2O_5/TiO_2 (1–6 wt%) and V_2O_5/Al_2O_3 (7.5–17.5 wt%) catalysts is observed at 685–725 and 750–760 K, respectively [22,23]. Thus, analysis of the reduction profiles of the *x*V90Ti–Al samples further suggests that the surface vanadia species coordinates with titania and alumina of the mixed oxide support. Based on the characterization studies, a schematic of the surface vanadia species in the supported catalysts calcined at 723 K is shown in Scheme 1.

3.2. Propane ODH reaction of supported vanadia catalysts

The catalytic activity of *x*V90Ti–Al was tested for propane ODH reaction by varying the contact time, and the results are shown in Fig. 7. Fig. 7 reveals that the propane conversion increases with an increase in contact time for each catalyst. At the same contact time, the propane conversion increases with an increase in vanadia loading: 2V90Ti–Al < 4V90Ti–Al < 7.5V90Ti–Al < 10V90Ti–Al. The increase in conversion with loading is expected since monolayer coverage has not been exceeded. The propene yield at iso-conversion also follows a similar trend as observed for the increase in propane conversion with vanadia loading at the same contact time.

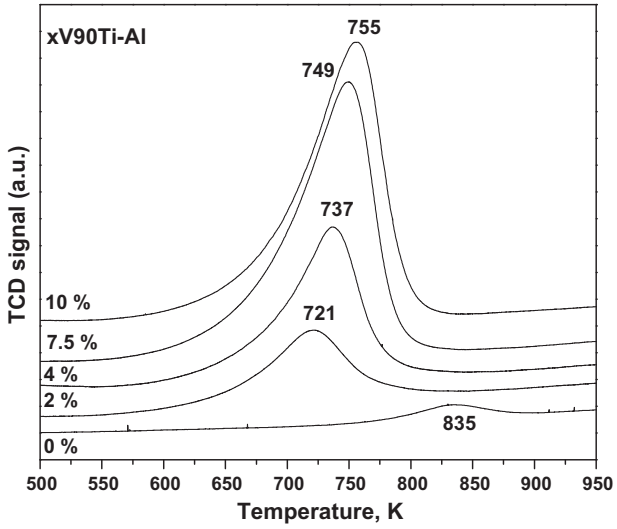

Fig. 6. TPR profiles of *x*V90Ti–Al catalysts (*x* = 0–10 wt%).

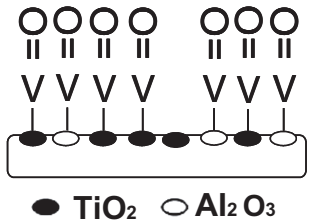

Scheme 1. Surface vanadia species anchored to titania and alumina in the mixed oxide support at 723 K.

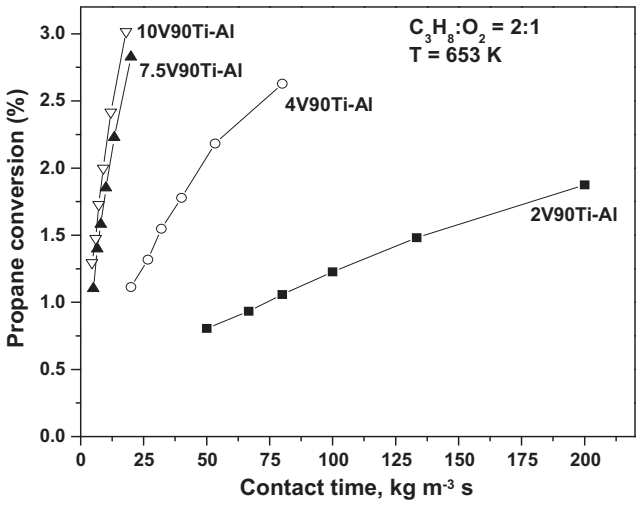

Fig. 7. Variation of propane conversion with contact time for the *x*V90Ti–Al (*x* = 2–10 wt%) catalysts.

Thus, the molecularly dispersed surface vanadia species behaves similar to other supported vanadia species on pure TiO_2 and Al_2O_3 supports [19].

Comparing the propane ODH reactivity of the 2V90Ti–Al and the comparable vanadia supported on TiO_2 (Degussa P-25) reveals that the activity is lower for the 2V90Ti–Al catalyst [24]. The lower activity of the 2V90Ti–Al catalyst for propane ODH reaction may be rationalized from the information obtained from characterization and previous propane ODH reaction studies. Characterization studies suggest that the vanadia phase is anchored to the titania and alumina phase of the mixed oxide support. Previous studies reveal that the vanadia phase is more active on titania than on alumina [8]. Thus, the 2V90Ti–Al catalyst, which has some of the surface vanadia species anchored to the titania and the rest to the less-active alumina phase, will possess a lower activity relative to the comparable vanadia supported on TiO_2 (Degussa, P-25).

3.3. Kinetic parameter estimation

Details of the reaction model and kinetic parameter estimation methodology are given elsewhere [19,20]. In this reaction model, the direct combustion of propane to carbon oxides is considered to be insignificant during the propane ODH reaction over supported vanadia catalysts [22,29,39]. The kinetic parameters associated with the propane ODH reaction were determined for the four catalysts using a simplified sequential Mars van Krevelen (MVK) reaction model considering propene and carbon oxides ($CO + CO_2$) as primary and secondary products, respectively. The MVK model assumes that the propane molecules react with lattice oxygen of the catalysts to produce propene molecules with a reaction rate of r_1, which then further react with lattice oxygen to produce carbon oxides with a reaction rate of r_2. The gas phase oxygen replenishes the lattice oxygen by re-oxidation of the reduced catalysts with a reaction rate of r_3. The rate equations of the three reactions rates, r_1, r_2 and r_3, are given below:

$$r_1 = k_1 P_{C_3H_8}(1-\beta) \quad (1)$$

$$r_2 = k_2 P_{C_3H_6}(1-\beta) \quad (2)$$

$$r_3 = k_3 P_{O_2}\beta \quad (3)$$

where k_i's (i = 1–3) are the rate constants in ml STP min^{-1} $(g\ cat)^{-1}$ atm^{-1}; P_i's are the partial pressures of the component, i, in atm; β is the degree of reduction of the catalyst and is the fraction of reduced sites to the total number of sites present.

Re-parameterization is required to overcome the correlation between the parameters and is achieved by reformulating the rate constants as

$$k_i = k_{io} \exp\left(\frac{-E_i}{R}\left(\frac{1}{T} - \frac{1}{T_m}\right)\right), \quad i = 1{-}3 \tag{4}$$

where k_{io}'s are the pre-exponential factors, ml STP min^{-1} (g cat)$^{-1}$ atm^{-1}; E_i's are the activation energies for the reaction i, kJ/mol; T is the actual reaction temperature, K; R is the universal gas constant, kJ (kmol)$^{-1}$ K; and T_m is the mean temperature, K.

The CO_2/CO ratios, ψ, required for the estimation of the kinetic parameters are calculated considering the entire reaction data set for each catalyst. With an increase in vanadia loading, the value of ψ decreases suggesting that the formation of CO_2 decreases as the vanadia loading is increased. The kinetic parameters, k_{io}'s and E_i's, with their units and the calculated standard error associated with each kinetic parameter are given in Table 2. Comparison of standard errors with parameter values suggests that the kinetic parameter values are estimated with a reasonable degree of accuracy. Moreover, a comparison between the actual and predicted concentration of all compounds analyzed reveals that a close correspondence exists for all the catalysts and is not shown here for brevity.

Comparison of various kinetic parameters presented in Table 2 reveals that the pre-exponential factor associated with the formation of propene increases with an increase in vanadia loading. The pre-exponential factor associated with the formation of carbon oxide formation also increases with an increase in vanadia loading. The activation energies for propene formation vary from 60 to 80 kJ mol^{-1}. The activation energies for carbon oxides formation are relatively constant till 7.5 wt% vanadia loading, and the 10V90Ti–Al catalyst possesses the highest value of activation energy for carbon oxides formation for this series of catalysts.

The propene yield for the different catalysts can be effectively compared by evaluating the lumped parameter k_1/k_2 [19,20]. For a series reaction, the propene yield determined at the same conversion is a function of k_1/k_2. Larger the value of k_1/k_2 higher is the propene yield at iso-conversion [40]. The value of k_1/k_2 ratio for various catalysts depends on the k_{10}/k_{20} ratio and difference in activation energies, $E_1 - E_2$. At $T = T_m$, the effect of activation energy is absent, and the k_1/k_2 and k_{10}/k_{20} ratios are equal. The values of k_{10}/k_{20} and $E_1 - E_2$ are also presented in Table 2 along with the kinetic parameter. The variation of the k_{10}/k_{20} ratio values reveals that as the vanadia loading is increased the k_{10}/k_{20} value increases till 7.5 wt% and then decreases for the 10 wt% loading sample suggesting that at a reaction temperature of 643.15 K ($T = T_m$) the propene yield at iso-conversion increases with vanadia loading and then decreases. Such a variation of propene yield with vanadia loading is indeed observed, except for the 10 wt% loading sample.

At reaction temperatures different from $T = T_m$, the $E_1 - E_2$ difference needs to be considered since this difference affects the k_1/k_2 variation with temperature. Since the $E_1 - E_2$ is positive, the k_1/k_2 values for all catalysts increase with temperature. The $E_1 - E_2$ values, however, decrease with an increase in vanadia loading suggesting that the k_1/k_2 value increases more significantly with temperature for lower loading sample compared to high loading catalysts. Despite the specific variations, the k_1/k_2 follows similar trends as k_{10}/k_{20} in the temperature range of the present study, except at high temperatures where the 7.5 wt% loading sample possesses the highest k_1/k_2 value. Comparison of the kinetic parameters and the propene yield versus conversion data reveals that there is a similarity in variation of the k_1/k_2 ratio and the propene yield at iso-conversion with vanadia loading. Furthermore, comparing the k_1/k_2 ratio at 653 K for the 2V90Ti–Al catalyst and the same vanadia loading on TiO_2 (Degussa P-25), 2VTi, reveals that the k_1/k_2 ratio is higher for the 2V90Ti–Al catalyst suggesting that at the same conversion the 2V90Ti–Al produces more propene [19]. At the same contact time, however, the propane conversion is higher for the 2VTi catalyst compared to the 2V90Ti–Al catalyst.

3.4. Effect of catalyst calcination temperature

To observe the effect of calcination temperature on the activity, the xV90Ti–Al samples calcined at different temperatures were tested for the propane ODH reaction at a common reaction temperature of 673 K. The propane to oxygen ratio of 2:1 and a flow rate of 75 ml/min were also kept constant. It was observed that the variation in catalytic activity with calcination temperature depends on the specific xV90Ti–Al sample. To understand the relative variation in activity with calcination temperature, the propene yields are normalized and shown in Fig. 8. The normalized propene yield at a reaction temperature of 673 K is achieved by dividing the propene yield achieved at a particular calcination temperature by the propene yield of the same catalyst calcined at 723 K. As shown in Fig. 8, the normalized propene yield for 2V90Ti–Al catalyst is relatively constant till a calcination temperature of 923 K and gradually increases for higher calcination temperatures. For the 4V90Ti–Al catalyst, the normalized propene yield increases with an increase in calcination temperature, reaches a maximum value at 923 K and decreases thereafter. The maximum propene yield at a calcination temperature of 923 K is about 3.5 times the propene yield of 4V90Ti–Al calcined at 723 K. For the 7.5V90Ti–Al catalyst, the propene yield slightly increases and then decreases, whereas for 10V90Ti–Al, the propene yield is initially constant and then decreases as the calcination temperature is increased. Similar variations are observed in the propane conversions.

To understand the unusual behavior of the 4V90Ti–Al catalyst, this sample was studied by DRIFT and XPS. The IR spectra of this dehydrated catalyst at different calcination temperatures are shown in Fig. 9 and reveal the presence of the V=O bond overtone vibration up to a calcination temperature of 923 K; the calcination temperature corresponding to the highest propene yield. The presence of the V=O bond overtone vibration indicates the presence of the surface vanadia molecularly dispersed species. Above a calcination

Table 2
Kinetic parameter values of the xV90Ti–Al catalysts. Standard errors are given in parentheses. T_m = 643.15 K.

Parameter	Units	Catalysts			
		2V90Ti–Al	4V90Ti–Al	7.5V70Ti–Al	10V90Ti–Al
k_{10}	ml STP min^{-1} (g cat)$^{-1}$ atm^{-1}	8 (0.2)	26 (2)	112 (5)	147 (2)
k_{20}		110 (4)	176 (18)	375 (38)	602 (7)
k_{30}		87 (4)	420 (42)	736 (90)	1555 (51)
k_{10}/k_{20}	–	0.07	0.15	0.30	0.25
E_1	kJ mol^{-1}	82 (2)	73 (5)	60 (6)	77 (2)
E_2		27 (3)	32 (6)	28 (4)	64 (1)
E_3		119 (11)	183 (16)	129 (21)	282 (10)
$E_1 - E_2$		55	41	32	13

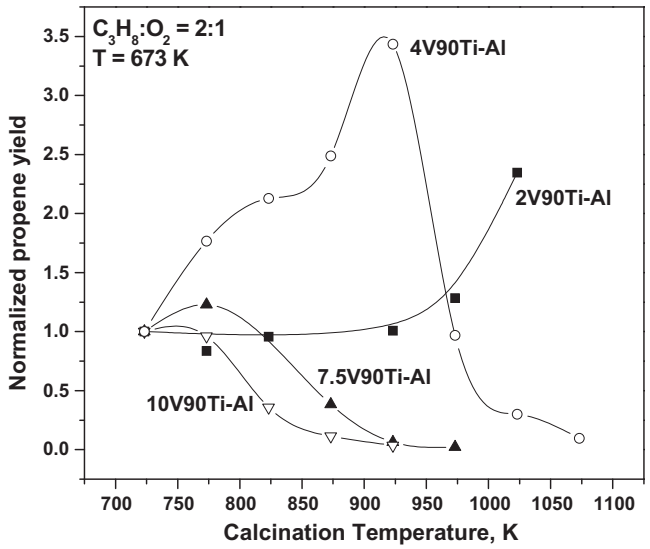

Fig. 8. Normalized propene yield versus calcination temperature for the *x*V90Ti–Al catalysts.

temperature of 923 K, the V=O bond intensity decreases indicating a loss of surface vanadia molecularly dispersed species [24]. Consequently, the propene yield is expected to decrease for the 4V90Ti–Al catalyst calcined at temperatures higher than 923 K, and this is indeed observed in Fig. 8. Thus, the decrease in catalytic activity at higher calcination temperatures is due to the loss of the surface vanadia active sites.

Explaining the increase in propene yield from DRIFT studies was not possible since the concentration of the surface vanadia molecularly dispersed species appears to be similar, which would suggest a similar catalytic activity. To investigate the reason for an increase in propene yield for the 4V90Ti–Al sample, XPS studies were undertaken on representative 90Ti–Al and 4V90Ti–Al samples calcined at different temperatures. These XPS results are shown in Table 3 in terms of the Al/Ti, V/Ti and V/Al atomic ratios. For the 90Ti–Al support, the Al/Ti atomic ratio increases with an increase in calcination temperature indicating that the surface is progressively enriched with alumina as the calcination temperature is increased. This change in surface concentration of mixed oxides

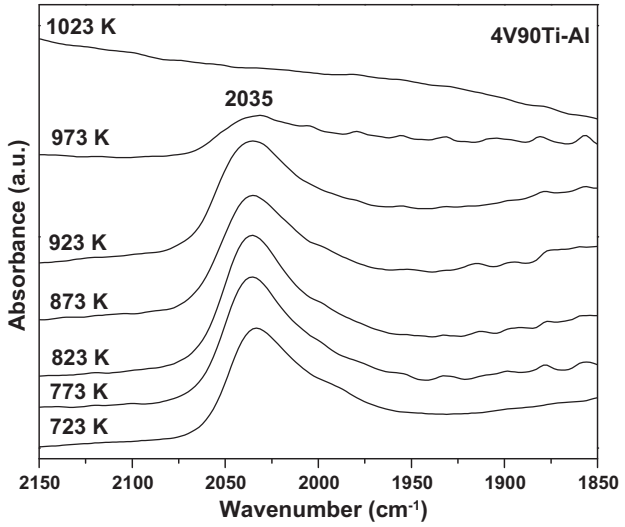

Fig. 9. DRIFT spectra of the 4V90Ti–Al sample calcined at different temperatures obtained under dehydrated conditions. Each spectrum was subtracted with the spectrum of 90Ti–Al support calcined at the corresponding temperature.

Table 3
Atomic ratio of Al/Ti, V/Ti and V/Al for the 90Ti–Al and 4V90Ti–Al catalysts calcined at different temperatures.

Sample	Calcination temperature (K)	Atomic ratio		
		Al/Ti	V/Ti	V/Al
90Ti–Al	723	0.010	0	0
	823	0.129	0	0
	923	0.148	0	0
	1023	0.211	0	0
4V90Ti–Al	723	0.848	0.079	1.80
	823	0.151	0.073	0.481
	923	0.090	0.103	1.151
	1023	0.279	0.219	0.785

has been attributed to the difference in surface free energy of the individual metal oxides that make up the mixed oxide support [41]. For the 4V90Ti–Al catalyst, however, a different Al/Ti atomic ratio variation with an increase in calcination temperature is observed. Except for the 4V90Ti–Al sample calcined at 1023 K, the Al/Ti atomic ratio decreases suggesting that the catalyst surface is progressively enriched with Ti. For these samples, which are calcined below 1023 K, the surface vanadia species is progressively more likely to be bonded to the titania phase and, hence, are progressively more active; explaining the higher propene yield for the 4V90Ti–Al catalysts at calcination temperatures below 1023 K. For the 4V90Ti–Al catalyst calcined at 1023 K, it appears that the surface vanadia species is lost most probably due to the formation of vanadium-based mixed oxide compounds, whose exact nature is unknown. In fact, the DRIFT spectra suggest that the loss of surface vanadia species in the 4V90Ti–Al sample starts at 973 K. Unfortunately, such a sample was not analyzed by XPS. Thus, for mixed oxide supported vanadium oxide catalysts, the calcination temperature is very important in obtaining the most active catalyst since the presence/absence of the surface-active phase, and the surface composition of the support strongly depends on the calcination temperature.

4. Conclusions

A 90Ti–Al support was synthesized by the sol–gel method and characterized. Using this 90Ti–Al support, several supported vanadia catalysts were prepared by the incipient wetness impregnation method and also characterized. The surface area of the 90Ti–Al support decreases with an increase in calcination temperature. The decrease in surface area of the specific supported vanadia catalysts depends on the vanadia loading and calcination temperature. The higher vanadia loading samples lose their surface area more readily compared to low vanadia loading samples.

Characterization studies reveal that the 90Ti–Al support calcined at 723 K possesses surface titania and alumina phase. Furthermore, the supported vanadia catalysts possess molecularly dispersed reducible surface vanadia species, and monolayer coverage is not exceeded. Analysis of the hydroxyl groups and reduction profiles suggests that the surface vanadia species is anchored to the alumina and titania phase of the support.

Propane ODH reaction studies reveal that the molecularly dispersed vanadia species on the mixed oxide support behave similar to other supported vanadia catalysts since the propane conversion increases with an increase in vanadia loading for these catalysts. The kinetic parameters associated with the propane ODH reaction also reveal similar trends in accordance with the increase in active surface vanadia sites. Another interesting feature of these catalysts is the effect of calcination temperature. With an increase in calcination temperature, the catalytic activity at 673 K varies depending on the specific catalyst. This variation in catalytic activity is

related to the surface composition, which depends on the calcination temperature. The calcination temperature determines the presence/absence of the surface vanadia species and the surface Al/Ti atomic ratio.

Acknowledgments

The authors are thankful to Prof. Israel E. Wachs and Dr. Kamalakanta Routray, Lehigh University, for providing the Raman spectra. The authors gratefully acknowledge the support from the Department of Science and Technology (DST), India.

Appendix A. Supplementary data

Supplementary data associated with this article can be found, in the online version, at doi:10.1016/j.jcat.2010.05.017.

References

[1] E.A. Mamedov, V.C. Corberan, Appl. Catal. A: Gen. 127 (1995) 1.
[2] G. Deo, I.E. Wachs, J. Haber, Crit. Rev. Surf. Chem. 4 (1994) 141.
[3] M. Sanati, A. Anderson, Ind. Eng. Chem. Res. 30 (1991) 320.
[4] G.C. Bond, S.F. Tahir, Appl. Catal. 71 (1991) 1.
[5] G. Ramis, G. Busca, P. Forzatti, Appl. Catal. B: Environ. 1 (1992) L9.
[6] J.P. Chen, R.T. Yang, Appl. Catal. A: Gen. 80 (1992) 135.
[7] B.M. Reddy, K.N. Rao, G.K. Reddy, P. Bharali, J. Mol. Catal. A: Chem. 253 (2006) 44.
[8] K. Routray, K.R.S.K. Reddy, G. Deo, Appl. Catal. A: Gen. 265 (2004) 103.
[9] B.M. Reddy, M.V. Kumar, E.P. Reddy, S. Mehdi, Catal. Lett. 36 (1996) 187.
[10] R.Y. Saleh, I.E. Wachs, S.S. Chan, C.C. Chersich, J. Catal. 98 (1986) 102.
[11] X. Gao, S.R. Bare, J.L.G. Fierro, M.A. Bañares, I.E. Wachs, J. Phys. Chem. B 102 (1998) 5653.
[12] J.B. Miller, E.I. Ko, Catal. Today 35 (1997) 269.
[13] O. Yamaguchi, Y. Mukaida, J. Am. Ceram. Soc. 72 (1989) 330.
[14] J. Yang, Y.X. Huang, J.M.F. Ferreira, J. Mater. Sci. Lett. 16 (1997) 1933.
[15] L.E. Depero, J. Solid State Chem. 104 (1993) 470.
[16] J. Ramirez, L. Ruiz-Ramirez, L. Cedeno, V. Harle, M. Vrinat, M. Breysse, Appl. Catal. A: Gen. 93 (1993) 163.
[17] W. Zhaobin, X. Qin, G. Xiexian, E.L. Sham, P. Grange, B. Delmon, Appl. Catal. 63 (1990) 305.
[18] G.M. Dhar, B.N. Srinivas, M.S. Rana, M. Kumar, S.K. Maity, Catal. Today 86 (2003) 45.
[19] D. Shee, T.V.M. Rao, G. Deo, Catal. Today 118 (2006) 288.
[20] K. Routray, G. Deo, AIChE J. 51 (2005) 733.
[21] R.P. Singh, M.A. Bañares, G. Deo, J. Catal. 233 (2005) 388.
[22] T.V.M. Rao, G. Deo, Ind. Eng. Chem. Res. 46 (2007) 70.
[23] T.V.M. Rao, G. Deo, AIChE J. 53 (2007) 1538.
[24] D. Shee, G. Deo, Catal. Lett. 124 (2008) 340.
[25] Y. Segura, L. Chmielarz, P. Kustrowski, P. Cool, R. Dziembaj, E.F. Vansant, J. Phys. Chem. B 110 (2006) 948.
[26] B. Mitra, I.E. Wachs, G. Deo, J. Catal. 240 (2006) 151.
[27] M.A. Vuurman, I.E. Wachs, A.M. Hirt, J. Phys. Chem. 95 (1991) 9928.
[28] I.E. Wachs, Catal. Today 27 (1996) 437.
[29] T.V.M. Rao, G. Deo, Catal. Comm. 8 (2007) 957.
[30] L.E. Depero, P. Bonzi, M. Musci, C.J. Casale, Solid State Chem. 111 (1994) 247.
[31] A. Khodakov, B. Olthof, A.T. Bell, E. Iglesia, J. Catal. 181 (1999) 205.
[32] I.E. Wachs, B.M. Weckhuysen, Appl. Catal. A: Gen. 157 (1997) 67.
[33] N. Magg, B. Immaraporn, J.B. Giorgi, T. Schroeder, M. Baumer, J. Dobler, Z. Wu, E. Kondratenko, M. Cherian, M. Baerns, P.C. Stair, J. Sauer, H.J. Freund, J. Catal. 226 (2004) 88.
[34] I.E. Wachs, Y. Chen, J.M. Jehng, L.E. Briand, T. Tanaka, Catal. Today 78 (2003) 13.
[35] G. Deo, F.D. Hardcastle, M. Richards, A.M. Hirt, I.E. Wachs, Novel materials in heterogeneous catalysis, in: R.T.K. Baker, L.L. Murrell (Eds.), ACS Symposium Series, vol. 437, American Chemical Society, Washington, DC, 1990, p. 317.
[36] H. Eckert, I.E. Wachs, J. Phys. Chem. 93 (1989) 6796.
[37] M.A. Vuurman, D.J. Stufkens, A. Oskam, G. Deo, I.E. Wachs, J. Chem. Soc. Faraday Trans. 92 (1996) 3259.
[38] M.A. Vuurman, I.E. Wachs, D.J. Stufkens, A. Oskam, J. Mol. Catal. 80 (1993) 209.
[39] K. Chen, A. Khodakov, J. Yang, A.T. Bell, E. Iglesia, J. Catal. 186 (1999) 325.
[40] H.S. Fogler, Elements of Chemical Reaction Engineering, third ed., Prentice-Hall of India Pvt. Ltd., New Delhi, 2002. p. 192.
[41] B.M. Reddy, B. Choudhury, E.P. Reddy, A. Fernandez, Langmuir 17 (2001) 1132.